Temperature dependence of the band gap of zinc nitride observed in photoluminescence measurements

A. Trapalis, I. Farrer, K. Kennedy, A. Kean, J. Sharman, and J. Heffernan

Citation: Appl. Phys. Lett. **111**, 122105 (2017); doi: 10.1063/1.4997153
View online: http://dx.doi.org/10.1063/1.4997153
View Table of Contents: http://aip.scitation.org/toc/apl/111/12
Published by the American Institute of Physics

Temperature dependence of the band gap of zinc nitride observed in photoluminescence measurements

A. Trapalis,[1] I. Farrer,[1] K. Kennedy,[1] A. Kean,[2,3] J. Sharman,[2] and J. Heffernan[1,a)]
[1]*Department of Electronic and Electrical Engineering, University of Sheffield, Wheeldon Street, Sheffield S3 7HQ, United Kingdom*
[2]*Johnson Matthey, Blount's Court, Reading RG4 9NH, United Kingdom*
[3]*NikaWorks Ltd., Watlington, Oxfordshire OX49 5JT, United Kingdom*

(Received 21 July 2017; accepted 8 September 2017; published online 20 September 2017)

We report the photoluminescence properties of DC sputtered zinc nitride thin films in the temperature range of 3.7–300 K. Zinc nitride samples grown at 150 °C exhibited a narrow photoluminescence band at 1.38 eV and a broad band at 0.90 eV, which were attributed to the recombination of free carriers with a bound state and deep-level defect states, respectively. The high-energy band followed the Varshni equation with temperature and became saturated at high excitation powers. These results indicate that the high-energy band originates from shallow defect states in a narrow bandgap. Furthermore, a red-shift of the observed features with increasing excitation power suggested the presence of inhomogeneities within the samples. [http://dx.doi.org/10.1063/1.4997153]

Zinc Nitride (Zn_3N_2) is a II-V semiconductor material whose properties are relatively little studied compared to materials used in commercial applications, such as III-V semiconductors. Because of the relative abundance of zinc compared to other metals and the use of non-toxic nitrogen, Zn_3N_2 is a candidate for the fabrication of low cost semiconductor devices such as low cost solar cells. However, further investigation of its basic material properties is necessary before the full potential of this material can be realized. The bandgap of Zn_3N_2 has been a controversial topic in published literatures,[1,2] with reports ranging from 0.9 to 3.5 eV. Even though this is a very wide range, similar discrepancies have been reported in the early stages of other materials. For instance, the bandgap of InN was initially reported to be as high as 2.3 eV, but in later studies,[3–7] it was found to have a much lower bandgap of 0.7 eV. Oxygen contamination was, among other effects, considered to be the cause behind the wide bandgap reports. Zn_3N_2 tends to oxidise at ambient conditions, which has complicated the unambiguous identification of its bandgap. For instance, in a previous paper, we showed that the range of optical properties between as-grown and fully oxidised films can explain the widely varying reports of the optical bandgap found in the literature.[8] In addition to oxidation, several other competing effects can also influence the bandgap, including Burstein-Moss shifts and composition variation.

Photoluminescence (PL) spectroscopy is used as a sensitive probe of band-to-band emissions, shallow and deep level impurities, and defect states. In addition, the overall material quality can be assessed through the photoluminescence yield and its temperature and excitation intensity dependence.[9,10] There have been only a few reports of photoluminescence in Zn_3N_2 films in the case of both narrow and wide bandgap sample types reported in the literature.[11,12] Furthermore, the temperature dependence of these bands has not been investigated fully, and photoluminescence studies have not to date shed light on the nature and size of the bandgap in Zn_3N_2. Wei *et al*. reported an irregular temperature dependence of photoluminescence in their Zn_3N_2 films, where the change in intensity of the features observed in their samples was not monotonic with temperature[12] and their spectral position did not shift with temperature. In another study, photoluminescence was not observed at all in monocrystalline films grown by MBE.[13] In this paper, we report on a detailed study of the photoluminescence properties of Zn_3N_2 films to further improve the understanding of this promising semiconductor material. Well defined bands were observed, and their emission energies were shown to follow the well-known Varshni equation for semiconductor bandgaps.

Zn_3N_2 films were grown on a heated glass substrate by DC sputtering of a Zn target in N_2 plasma in a Denton Vacuum Explorer. Samples were grown at 150 °C, a N_2 flow rate of 45 SCCM, and a sputter power of 85 W. The physical and optical properties of samples grown on the same system are examined in detail in a previous publication.[8] Photoluminescence (PL) measurements were performed with the sample mounted on a copper plate inside an Oxford Instruments Optistat Dry cryostat. The cryostat chamber was pumped down to 10^{-4} mbar and subsequently cooled down to 3.7 K using a closed-circuit liquid He compressor. The sample was excited using a 100 mW 642 nm laser. A variable neutral density filter was used to attenuate the power of the excitation beam. The emitted light was collected from the surface of the sample and focused into an Andor 500i spectrometer which enabled measurements in the spectral range of 600–1600 nm.

The XRD pattern and an SEM image of a typical sample are shown in Fig. 1. The XRD measurements revealed diffraction peaks associated with the Zn_3N_2 anti-bixbyite

a)Author to whom correspondence should be addressed: jon.heffernan@sheffield.ac.uk

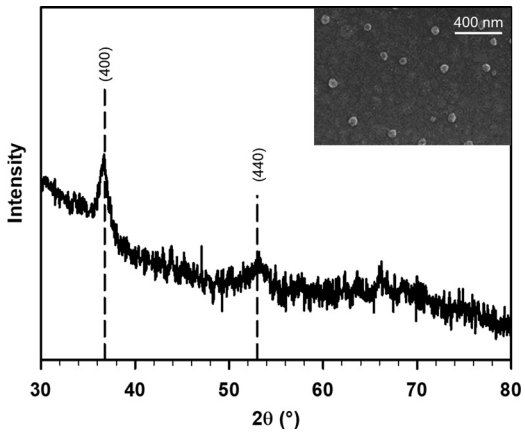

FIG. 1. XRD pattern of a sample grown at 150 °C. Inset: SEM image of the same sample.

crystal structure. The XRD pattern suggests that samples grown at these conditions are (100)-oriented because of the dominance of the (400) diffraction peak. However, the relatively broad peaks observed suggest a large distribution of lattice sizes, likely due to strain and defects.

The temperature dependent PL spectra are shown in Fig. 2. The spectrum at T = 3.7 K featured a narrow band at 1.44 eV (band A) and a second band (band B) on the low energy side of band A. With increasing temperature, the intensity of band A decreased and its position shifted to 1.38 eV at T = 300 K. The efficiency of band B decreased rapidly with increasing temperature, and it could not be resolved at elevated temperatures. In addition to PL measurements, the optical bandgap of the sample was identified as 1.43 eV based on the absorption coefficient calculated from reflectivity and transmission measurements at room temperature.[8] Therefore, it is evident from the PL measurements that the sample exhibited a photoluminescence band near the absorption onset at room temperature. Furthermore, the temperature dependence of band A, which is the highest energy band observed, matches the profile of band to band transitions. The observed red-shift with increasing temperature follows the well-known Varshni equation, which empirically describes the effect of thermal vibrations on the bandgap of semiconductors.[9,10] Band A also exhibits a high-energy tail, more clearly observed at T = 300 K, which is

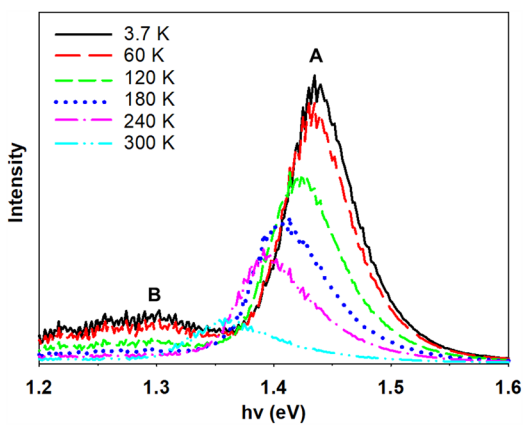

FIG. 2. Temperature dependent PL of a sample shortly after growth with an excitation power of 30 mW.

indicative of transitions that involve the recombination of free carriers[10] and correlates with a high n-type carrier density of $\sim 10^{19}\,cm^{-3}$ found in these samples through Hall measurements. The high carrier density is thought to originate from native defects in the samples as observed generally in Zn_3N_2.[14,15]

Since much of the debate over the bandgap of Zn_3N_2 is based on the possible effects of oxidation, we investigated the effect of ambient oxidation on PL. PL measurements of the same sample after prolonged exposure to ambient air are shown in Fig. 3(a). The repeated measurements revealed the presence of a low-energy broad band at 0.90 eV (band C), in addition to bands A and B which were initially observed. The intensity of band C decreased with increasing temperature; however, its position did not shift. Bands A and B behaved similarly to the original measurements. The very large width and the poor temperature dependence of band C suggest that it is related to deep-level defects. Wei *et al.* observed a similar band and concluded that it is caused by deep levels introduced by oxygen contamination.[12] A closer comparison of the spectra before and after prolonged exposure to ambient, shown in Fig. 3(b), clearly showed that band A had blue-shifted and decreased in intensity in comparison to the original measurement. The decrease in the intensity of band A with time suggests that the sample had been partially oxidised resulting in decreased PL efficiency. Furthermore, the blue-shift of band A indicates the presence of regions with a wider bandgap within the sample.

To provide more information on the origin of the observed high-energy bands, power dependent PL was performed at both low and high temperatures. The spectra in Figs. 4(a) and 4(b) show low and room temperature measurements for different excitation powers. A red-shift in the emission energies of bands A and B was observed as the excitation power increased. Band C, which is not shown here, displayed a similar shift. Furthermore, the relative intensities of bands A and B changed significantly with excitation power. The intensities and emission energies of bands A and B at 3.7 and 294 K are plotted as a function of excitation power in Figs. 4(c) and 4(d). At low excitation powers, band B was more efficient than band A, but at higher

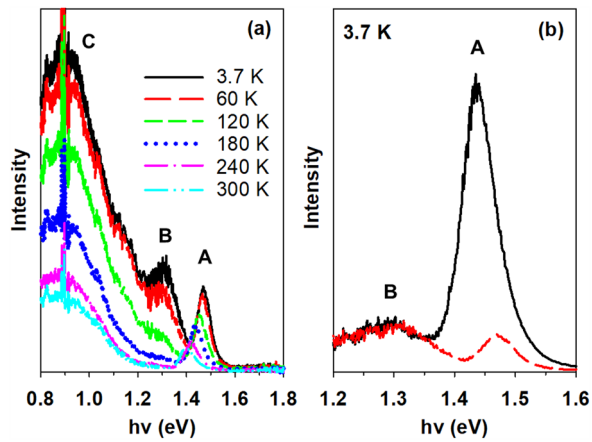

FIG. 3. (a) Temperature dependent PL of the zinc nitride sample after prolonged exposure to ambient. (b) Comparison of the high-energy bands of the same sample before (solid) and after (dashed) prolonged exposure to ambient.

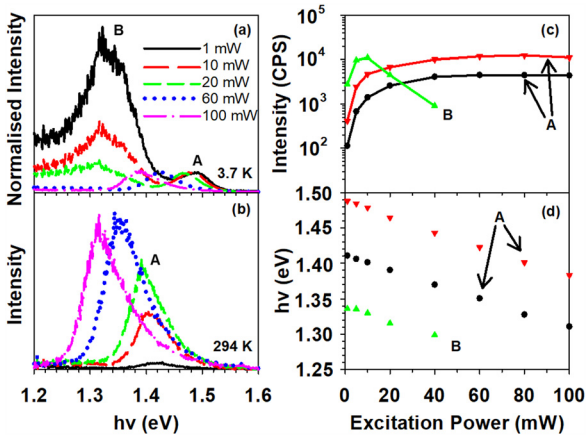

FIG. 4. PL spectra of bands A and B at (a) 3.7 and (b) 294 K at different excitation powers. (c) Peak intensities and (d) emission energies of band A at 294 K (•) and bands A (inverted filled red triangle) and B (filled green triangle) at 3.7 K as a function of excitation power. The spectra in (a) have been normalised at the maximum intensity of band A.

excitation powers, it deteriorated to the point where it could no longer be resolved, while band A became saturated. The shift of the emission energies with excitation power was linear and occurred at a similar rate for both bands.

The saturation of band A with excitation power suggests that the recombination process involves a transition from or to a bound donor or acceptor state. At high excitation powers, these bound states are fully populated, resulting in a saturation of the PL intensity.[10] On the other hand, the observed red-shift with increased excitation power is more unusual. Such an effect may be observed in a Type-II transition, when high-energy photogenerated carriers overflow to nearby bands and subsequently relax to lower energy conduction band valleys. However, density of states calculations for Zn_3N_2 show no evidence for such a band alignment.[16–18] Furthermore, the red-shift is too significant to be exclusively caused by the thermal effect. Instead, we suggest that the observed shift with excitation power is related to inhomogeneities in the sample. Defects may be introduced in oxygen-doped or strained regions in the films which have a different conduction band minimum than the rest of the film. As the excitation power is increased, the photogenerated carriers are activated and become more mobile, allowing them to relax to lower energy states. As a result, a red-shift is observed with increased excitation intensity. Prasada Rao *et al*. have observed similar behaviour in ZnO PL and attributed it to a high concentration of intrinsic defects.[19] Similarly, we suggest that this effect is related to structural defects and impurities specific to these samples. After further exposure to ambient, the samples became increasingly non-uniform and only emitted light from certain regions with a similar power dependence.

The relative integrated intensities (I/I_0) of bands A and B at excitation powers of 1 and 100 mW are shown in Fig. 5(a). It is noticed that the thermal quenching of band A is offset to higher temperatures when excited with a power of 100 mW. This is an indication of heating caused by the laser, which affected the measurement of I_0 at the lowest temperatures and can, to some extent, be expected at high excitation powers. The temperature dependent intensities of these

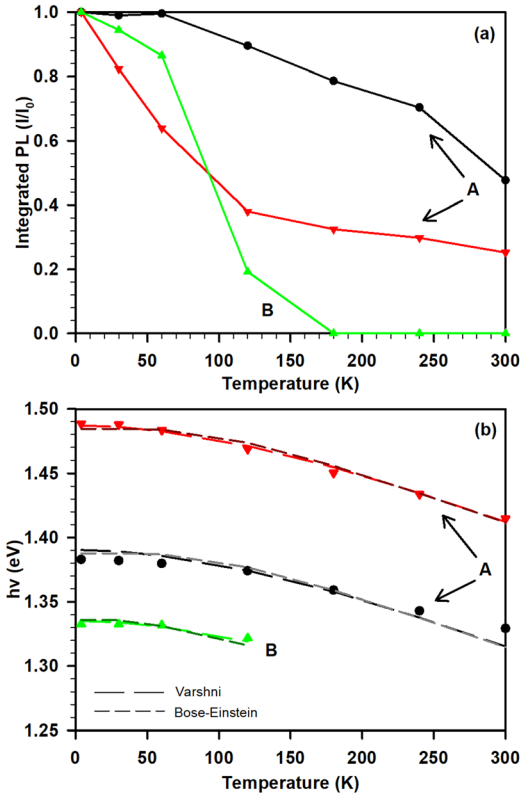

FIG. 5. Temperature dependence of (a) relative integrated intensities (I/I_0) and (b) the emission energies of band A at an excitation power of 100 mW (•) and bands A (inverted filled red triangle) and B (filled green triangle) at an excitation power of 1 mW.

bands were used in an attempt to calculate the activation energies (E_A) of the defects associated with these transitions, using the following equation:[20]

$$\frac{I}{I_0} = \frac{1}{1 + \alpha_1 \exp\left(-\frac{E_{A_1}}{kT}\right) + \alpha_2 \exp\left(-\frac{E_{A_2}}{kT}\right)}. \quad (1)$$

From this analysis, the thermal quenching of band A was fitted more closely using two competitive non-radiative centres with activation energies of 50 and 5 meV. In contrast, the thermal quenching of band B was fitted with a lower activation energy of 36 meV. While the origin of these activation energies is currently not understood, the calculations are mentioned for future reference.

The emission energies of bands A and B at excitation powers of 1 and 100 mW are shown as a function of temperature in Fig. 5(b). To evaluate the temperature dependence of these bands, the data were fitted to the Varshni equation, $E_g(T) = E_{g_0} - aT^2/(T+\beta)$, and a Bose-Einstein function,[21,22]

$$E_g(T) = E_{g_0} - \frac{2a_B}{\exp\left(\frac{\Theta_E}{T}\right) - 1}. \quad (2)$$

The dashed lines in Fig. 5(b) show fits of the data with each function. The fitting parameters were $\alpha = 5.92 \times 10^{-4}$ eV/K and $\beta = 409.9$ K for the Varshni equation and $\alpha_B = 65$ meV and $\Theta_E = 305.8$ K for the Bose-Einstein function. The Debye temperature of the material, calculated as $\Theta_D = 4\Theta_E/3$, is

approximately 408 K. This is in good agreement with the Varshni parameter β, which is often related to the Debye temperature. However, these values are significantly lower than the computationally calculated value of ~610 K by Li *et al.*[23] While care must be taken in the use of these equations with PL results, the close fit and the fitting parameters, which are similar to other semiconductors such as GaAs,[24,25] suggest again that the bands observed in this study originate from shallow defects in a narrow band-gap semiconductor. Other effects such as conduction band filling, band tail states, unintentional oxygen contamination, and strain may still influence the observed bandgap, potentially making it wider.[26,27] The significance of such effects remains to be investigated. However, we believe that the observation of PL which exhibits a temperature dependence typical of band to band transitions strongly suggests that the intrinsic bandgap of Zn_3N_2 is in the energy region of 1.40 eV and ultimately sheds some light on the bandgap controversy surrounding Zn_3N_2.

In summary, we have studied the photoluminescence of polycrystalline Zn_3N_2 films. Samples grown on a heated substrate displayed narrow PL features around 1.40 eV which were attributed to recombination in shallow donor or acceptor states with activation energies of 50 and 5 meV. The temperature dependence of the bandgap of Zn_3N_2 was observed by studying these bands at low temperatures which were shown to follow the empirical Varshni equation in a manner that is comparable to other semiconductors. The authors believe that the results strongly suggest that Zn_3N_2 is intrinsically a narrow bandgap material. A red-shift of the high-energy bands with increased excitation power was attributed to inhomogeneities due to defects in the crystal structure.

The authors wish to acknowledge funding by the EPSRC (Engineering and Physical Science Research Council) and Johnson Matthey PLC (Award No. 14550005). The financial support by these parties is highly appreciated. The data presented in this paper are available to download for free with the following DOI: 10.15131/shef.data.c.3830899.

[1]T. Yang, Z. Zhang, Y. Li, M. Lv, S. Song, Z. Wu, J. Yan, and S. Han, Appl. Surf. Sci. **255**, 3544 (2009).
[2]S. Simi, I. Navas, R. Vinodkumar, S. R. Chalana, M. Gangrade, V. Ganesan, and V. P. M. Pillai, Appl. Surf. Sci. **257**, 9269 (2011).
[3]V. Y. Davydov, A. A. Klochikhin, R. P. Seisyan, V. V. Emtsev, S. V. Ivanov, F. Bechstedt, J. Furthmüller, H. Harima, A. V. Mudryi, J. Aderhold, O. Semchinova, and J. Graul, Phys. Status Solidi B **229**, r1 (2002).
[4]J. Wu, J. Appl. Phys. **106**, 011101 (2009).
[5]J. Wu, W. Walukiewicz, K. M. Yu, J. W. Ager III, E. E. Haller, H. Lu, W. J. Schaff, Y. Saito, and Y. Nanishi, Appl. Phys. Lett. **80**, 3967 (2002).
[6]T. Matsuoka, H. Okamoto, M. Nakao, H. Harima, and E. Kurimoto, Appl. Phys. Lett. **81**, 1246 (2002).
[7]J. Wu, W. Walukiewicz, W. Shan, K. M. Yu, J. W. Ager III, S. X. Li, E. E. Haller, H. Lu, and W. J. Schaff, J. Appl. Phys. **94**, 4457 (2003).
[8]A. Trapalis, J. Heffernan, I. Farrer, J. Sharman, and A. Kean, J. Appl. Phys. **120**, 205102 (2016).
[9]G. D. Gilliland, Mater. Sci. Eng.: R: Rep. **18**, 99 (1997).
[10]I. Pelant and J. Valenta, *Luminescence Spectroscopy of Semiconductors* (Oxford University Press, 2012).
[11]F. Zong, H. Ma, J. Ma, W. Du, X. Zhang, H. Xiao, J. Feng, and C. Xue, Appl. Phys. Lett. **87**, 233104 (2005).
[12]P.-C. Wei, S.-C. Tong, C.-M. Tseng, C.-C. Chang, C.-H. Hsu, and J.-L. Shen, J. Appl. Phys. **116**, 143507 (2014).
[13]W. Peng, T. Tiedje, H. Alimohammadi, V. Bahrami-Yekta, M. Masnadi-Shirazi, and W. Cong, Semicond. Sci. Technol. **31**, 10LT01 (2016).
[14]G. Z. Xing, D. D. Wang, B. Yao, L. F. N. A. Qune, T. Yang, Q. He, J. H. Yang, and L. L. Yang, J. Appl. Phys. **108**, 083710 (2010).
[15]M. Futsuhara, K. Yoshioka, and O. Takai, Thin Solid Films **322**, 274 (1998).
[16]S.-H. Yoo, A. Walsh, D. O. Scanlon, and A. Soon, RSC Adv. **4**, 3306 (2014).
[17]N. Jiang, J. L. Roehl, S. V. Khare, D. G. Georgiev, and A. H. Jayatissa, Thin Solid Films **564**, 331 (2014).
[18]Y. Kumagai, K. Harada, H. Akamatsu, K. Matsuzaki, and F. Oba, Phys. Rev. Appl. **8**, 014015 (2017).
[19]T. Prasada Rao, G. K. Goswami, and K. K. Nanda, J. Appl. Phys. **115**, 213513 (2014).
[20]M. Leroux, N. Grandjean, B. Beaumont, G. Nataf, F. Semond, J. Massies, and P. Gibart, J. Appl. Phys. **86**, 3721 (1999).
[21]L. Viña, S. Logothetidis, and M. Cardona, Phys. Rev. B **30**, 1979 (1984).
[22]B. Pejova, B. Abay, and I. Bineva, J. Phys. Chem. C **114**, 15280 (2010).
[23]Z. Li, P. Wang, H. Chen, and X. Cheng, Phys. B: Condens. Matter **406**, 1182 (2011).
[24]Y. P. Varshni, Physica **34**, 149 (1967).
[25]J. L. Shay, Phys. Rev. B **4**, 1385 (1971).
[26]V. Tiron and L. Sirghi, Surf. Coat. Technol. **282**, 103 (2015).
[27]H. Gao, X. Zhang, Y. Zhao, and B. Yan, AIP Adv. **7**, 025111 (2017).